

# Molecularly Imprinted MXene-Based Biosensor for Selective and Sensitive Bilirubin Detection

Sahil Dahiya

M.Sc Student  
Department of Chemistry  
All India Jat Heros Memorial College, Rohtak.

## Abstract:

The development of a reliable sensor requires integrating a suitable sensing platform with an efficient bio-recognition element. In this work, MXene was employed as the sensing platform and molecular imprinting as the bio-recognition strategy. This design enhanced both sensitivity and shelf life by avoiding enzymes, antibodies, or other biological molecules as receptors. Bilirubin-imprinted cavities exhibited high selectivity for bilirubin detection in human serum and synthetic samples, achieving a limit of detection (LOD) of 0.002 mg/dL, a sensitivity of  $69.6 \mu\text{A} (\log(\text{mg/dL})^{-1})\text{cm}^{-2}$ , and a limit of quantification (LOQ) of 6.6 mg/dL. With a relative standard deviation (RSD) of 1.2%, the sensor showed excellent inter- and intra-day repeatability. However, stability was limited to 30 days due to pristine MXene's tendency to oxidize and agglomerate from surface –OH groups. Future improvements may involve MXene-based composites for enhanced stability and conductive monomers such as pyrrole to optimize molecular imprinting and sensor performance.

**Keywords:** Bio-Sensor, Bilirubin Detection, LOD, MXene.

## I. INTRODUCTION

Bilirubin (BR) is an important biomarker used to assess liver dysfunction and diagnose many diseases, including jaundice, hepatitis, and biliary disorders. Accurate and sensitive detection of BR is critical because its concentration in biological fluids is low, and elevated levels of BR may lead to various health complications. The conventional detection methods are precise but cumbersome and expensive, and the sample processing is time-consuming. Against this backdrop, a biosensor's simplicity, high sensitivity, and cost-effectiveness have become highly important. Molecularly imprinted polymer (MIP) has been known to be specific and stable, with great promise in selective BR recognition. The integration of advanced nanomaterials like MXene to enhance the performance of MIP-based biosensors has gained vast attention. Recently, numerous reports have discussed the exceptional properties of MXene that have rendered it to be used as a functional material in electronics, sensors, energy storage devices, etc. [65], [98], [170]. Since, MXene presents excellent electrical, chemical, and thermal stability, offers high specific surface area, and exhibits favorable electrochemical properties, which in turn can be helpful in the fabrication of sensitive sensing interface, in the present study; Ti<sub>3</sub>C<sub>2</sub>T<sub>x</sub>MXene-modified ITO electrode is used to detect the BR by using electrochemical sensor based on MIP technique. Since Ti-3C<sub>2</sub>T<sub>x</sub>MXene is a good candidate for electrochemical application, it enhances the sensor sensitivity and is used to modify electrodes before polymerization. Also, when MXene is combined with o-phenylenediamine (o-PD), a monomer that readily polymerizes to form a robust and selective matrix, MXene creates a synergistic effect that can improve the stability, binding efficiency, and electron transfer rate of the biosensor. In addition, the specific structural and functional characteristics of MXene allow for stronger interactions with o-PD and improve the template binding sites during MIP formation. This new combination provides an effective approach to designing a sensitive, selective, and reliable platform for BR detection, thereby overcoming the constraints of conventional methods, and advancing biomedical diagnostics.

In this study, initially, 2D hierarchical  $Ti_3C_2TxMXene$  is synthesized by removing aluminum (Al) from titanium aluminium carbide ( $Ti_3AlC_2$  MAX phase as a precursor) with HCl and LiF as an etchant. The formation of  $Ti_3C_2TxMXene$  is confirmed by UV-Vis, XRD, and FESEM. Afterward, MIP is electropolymerized on a  $Ti_3C_2TxMXene$ -modified electrode using the cyclic voltammetry (CV) method in a sodium acetate buffer solution containing o-PD as the monomer and BR as template molecules, with the optimized number of scan cycles at a 100 mV/s scan rate. The BR-imprint is formed by washing the prepared MIP electrode with optimized solvent for a specific time. The prepared MXene/MIo-PD electrode at every modification step is characterized by FESEM and electrochemical techniques such as DPV, EIS, and CV. Finally, the designed electrode is used for BR sensing in synthetic and human serum. With a low detection limit and extreme stability, the designed MIP electrode successfully detects BR. Figure 1, presents the schematic representation of the steps involved in the sensor. For comparison studies, a non-molecularly imprinted polymer (NIP) electrode is also fabricated by the same process as the MIP electrode but without BR

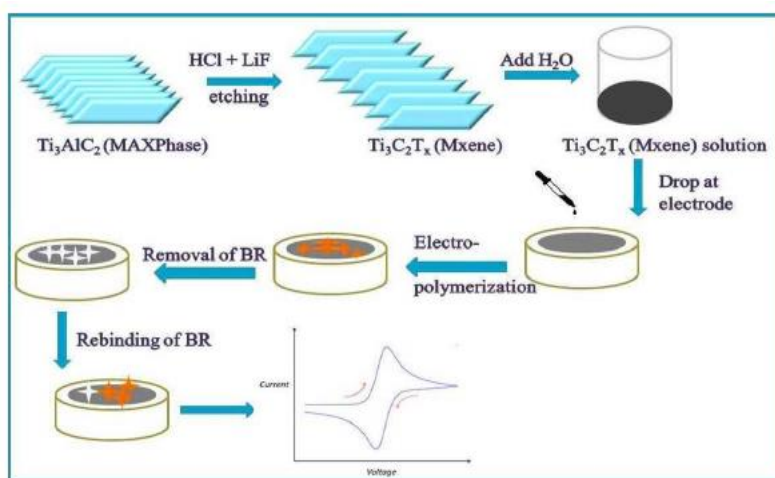


Figure 1: Synthesis of  $Ti_3C_2TxMXene$  and preparation of  $Ti_3C_2TxMXene$ -modified molecularly imprinted electrochemical sensor.

## II. EXPERIMENTAL SECTION

$Ti_3AlC_2$  (MAX phase; particle size 40-60  $\mu m$ ; purity 99%) is purchased from Nanoshel. Lithium fluoride (LiF), bilirubin (BR), o-phenylenediamine (o-PD), sodium acetate trihydrate, glacial acetic acid, uric acid (UA), dopamine (DA), galactose (GAL), and ascorbic acid (AA) are purchased from Sisco Research Laboratories Pvt. Ltd. (SRL).

For the preparation of phosphate buffer (0.1M, pH 7), sodium phosphate dibasic and sodium phosphate monobasic are purchased from CDH Chemicals. Potassium hexacyanoferrate (III) ( $K_3Fe(CN)_6$ ), potassium ferrocyanide ( $K_4Fe(CN)_6 \cdot 3H_2O$ ) and potassium chloride (KCl) are purchased from Fisher Scientific. All other analytical-grade chemicals are used without further purification. The electrochemical characterizations are conducted on an Autolab PGSTAT204 potentiostat/galvanostat (Eco Chemie, The Netherlands) using a three-electrode system. In this study, ITO is used as the working electrode, Ag/AgCl as the reference electrode, and Platinum foil as the counter electrode.

$Ti_3C_2TxMXene$  is prepared by the chemical etching method with a little modification [171]. The aluminium layer from  $Ti_3AlC_2$  is etched out by using LiF and HCl as an etchant. Initially, LiF (1.6 g) is added to 20 mL of 9 M HCl, followed by stirring at room temperature. When LiF in the HCl solution is completely dissolved, 1 g of  $Ti_3AlC_2$  is added over 30 minutes and continually stirred for 24 hours at 40°C. After the reaction, the obtained product is centrifuged at 3500 rpm several times in ultra-pure distilled water until the supernatant liquid pH reaches 6. Finally, the product is collected and vacuum-dried at 120°C for 18 hours. The prepared MXene is stored in powder form in the refrigerator for further use.

### III. RESULT & DISCUSSION

The synthesized MXene is characterized by FESEM, XRD, and UV-Vis absorption spectroscopy. The surface morphology of the MAX phase and synthesized MXene is seen with FESEM and presented in Figures 2 (a) and (b). The crystal structure of the precursor phase (MAX phase) is generally hexagonal with space group P63/mmc. The M-X makes an octahedral structure that is sandwiched between ‘A’ layers [13]. The MAX phase has a smooth surface, and layers are set as crystal rock. The removal of the “Al” layer from its MAX phase ( $Ti_3AlC_2$ ) during the etching process increases the space between the layers that can be seen by FESEM image of synthesized MXene. The single layers of MXene are also observed because of the complete removal of the “Al” layers. The side view of MXene with a freely loaded “accordion” arrangement specifies the happening of the etching process, and a few flakes are obtained on the MXene surface, which clarifies the successful partition of MXene layers from the stack [133].

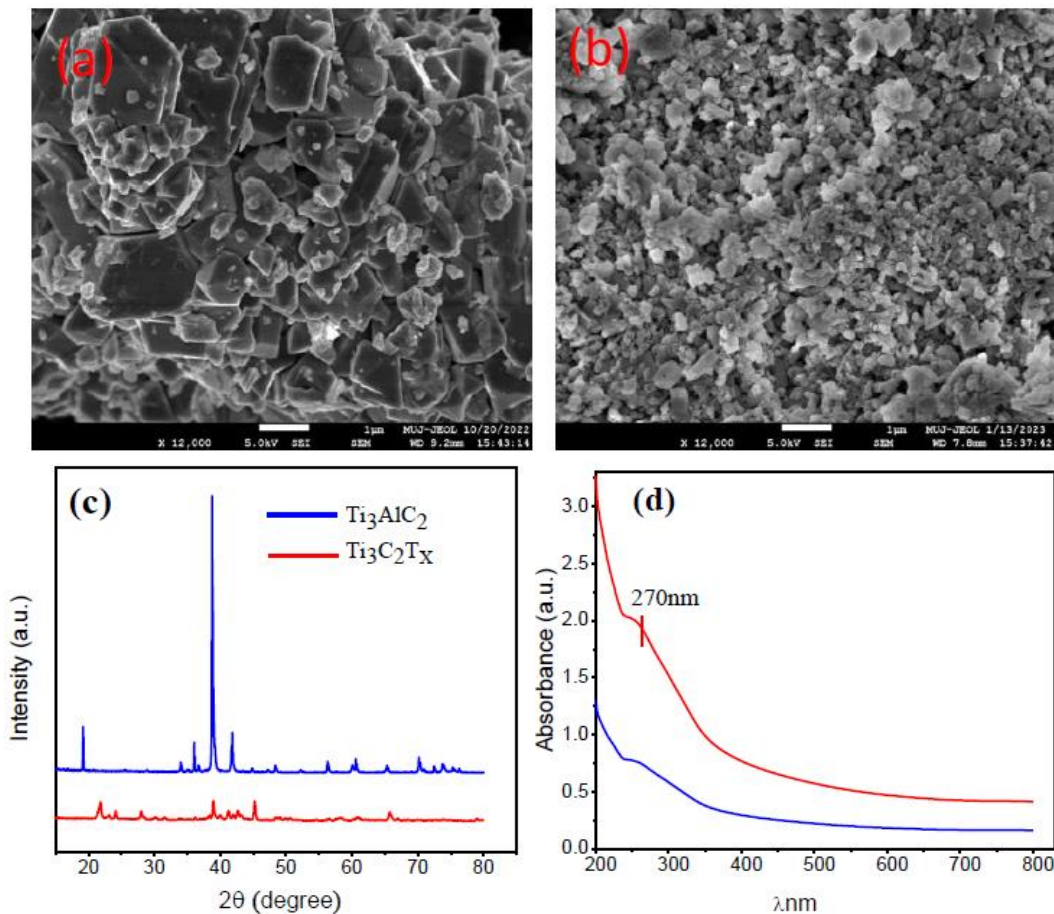


Figure 2: FESEM images of (a)  $Ti_3AlC_2$  MAX phase, (b)  $Ti_3C_2Tx$  MXene as synthesized at 12,000 magnifications, (c) XRD analysis, and (d) UV-Vis for  $Ti_3AlC_2$  and  $Ti_3C_2Tx$ .

The XRD analysis is carried out for structure characterization. The XRD data, as shown in Figure 2 (c), verify the successful synthesis of 2D  $Ti_3C_2Tx$ MXene. There is a decrease in intensity of the (104) peak at  $39^\circ$ , which shows the removal of the Al layer and the presence of terminal functional groups (-O, -OH, -F). Multiple peaks in the data show that MXene is polycrystalline in nature. The shift and broadening of various peaks are due to the presence of water in the MXene film during the filtration process. These are similar to the results reported in the literature [13]. The UV-Visible absorption spectrum of  $Ti_3C_2Tx$ MXene, as shown in Figure 2 (d), is also recorded to examine the optical properties of MXene. The absorption peak at 270 nm validates the synthesis of MXene.

#### IV. CONCLUSION

The BR-imprinted cavities are found to be selective for the specific sensing of BR molecules in human serum and synthetic samples, with a LOD of 0.002 mg/dL, a sensitivity of 69.6  $\mu\text{A} (\log(\text{mg/dL})-1)\text{cm}^{-2}$ , and LOQ of 6.6 mg/dL for the designed sensor. With RSD values of 1.2%, the prepared sensor showed good inter-day and intra-day repeatability. However, the prepared electrode has shown stability for only 30 days, a limitation attributed to the inherent instability of pristine MXene. The presence of hydroxyl (-OH) groups on the MXene surface leads to oxidation under ambient conditions, and the agglomeration of MXene layers further compromises its performance.

To overcome these challenges, future improvements could include the development of MXene-based composites to enhance stability and prevent agglomeration. Additionally, exploring alternative monomers like pyrrole, due to their conductive nature, may facilitate better MIP formation and improve the electrode's overall performance.

#### REFERENCES:

1. N. Méndez-Sánchez, L. Vítek, N. E. Aguilar-Olivos, and M. Uribe, "Bilirubin as a Biomarker in Liver Disease," in *Biomarkers in Liver Disease*, 1st ed. Dordrecht, Springer, 2016, pp. 1–25.
2. S. Kumbhar, M. Musale, and A. Jamsa, "Bilirubin metabolism: delving into the cellular and molecular mechanisms to predict complications," *Egyptian Journal of Internal Medicine*, vol. 36, no. 1, pp. 34, 2024.
3. M. M. Ramírez-Mejía, S. M. Castillo-Castañeda, S. C. Pal, X. Qi, and N. Méndez-Sánchez, "The Multifaceted Role of Bilirubin in Liver Disease: A Literature Review," *Journal of Clinical and Translational Hepatology*, vol. 000, no. 000, pp. 000–000, 2024.
4. Taurino, V. Van Hoof, A. Magrez, L. Forró, G. De Micheli, and S. Carrara, "Efficient voltammetric discrimination of free bilirubin from uric acid and ascorbic acid by a CVD nanographite-based microelectrode," *Talanta*, vol. 130, pp. 423–426, 2014.
5. L. Vitek, T. D. Hinds, D. E. Stec, and C. Tiribelli, "The physiology of bilirubin: health and disease equilibrium," *Trends in Molecular Medicine*, vol. 29, no. 4, pp. 315–328, 2023.
6. M. Kaplan, R. Bromiker, and C. Hammerman, "Hyperbilirubinemia, hemolysis, and increased bilirubin neurotoxicity," *Seminars Perinatology*, vol. 38, no. 7, pp. 429–437, 2014.
7. R. Guerra Ruiz et al., "Measurement and clinical usefulness of bilirubin in liver disease," *Advance in Laboratory Medicine*, vol. 2, no. 3, pp. 352–361, 2021.
8. Y.-Y. Huang, M.-J. Huang, H.-L. Wang, C.-C. Chan, and C.-S. Huang, "Bilirubin concentrations in thalassemia heterozygotes in university students," *European Journal of Haematology*, vol. 86, no. 4, pp. 317–323, 2011.
9. N. A. A. Al-Dahhan, H. A. A. Al-Dahhan, and B. J. Hussein, "Elevated bilirubin level increase the risk of gallstone disease in pediatric hereditary spherocytosis patients: A case report," *Systematic Reviews in Pharmacy*, vol. 11, no. 6, pp. 341–346, 2020.
10. L. B. VanWagner and R. M. Green, "Evaluating Elevated Bilirubin Levels in Asymptomatic Adults," *JAMA*, vol. 313, no. 5, p. 516, 2015.
11. R. L. Watson, "Hyperbilirubinemia," *Critical Care Nursing Clinics of North America*, vol. 21, no. 1, pp. 97–120, 2009.
12. G. F. Hoffmann and P. McKiernan, "Liver Disease," in *Inherited Metabolic Diseases*, Berlin, Heidelberg, Springer, 2017, pp. 203–226.
13. B. O. Olusanya, M. Kaplan, and T. W. R. Hansen, "Neonatal hyperbilirubinaemia: a global perspective," *Lancet Child and Adolescent Health*, vol. 2, no. 8, pp. 610–620, 2018.
14. W. Wolkoff and P. D. Berk, "Bilirubin Metabolism and Jaundice," in *Schiff's Diseases of the Liver*, Wiley, 2017, pp. 103–134.
15. T. Doumas et al., "Candidate reference method for determination of total bilirubin in serum: development and validation," *Clinical Chemistry*, vol. 31, no. 11, pp. 1779–1789, 1985.

16. N. Dhungana, C. Morris, and M. D. Krasowski, "Operational impact of using a vanadate oxidase method for direct bilirubin measurements at an academic medical center clinical laboratory," *Practical Laboratory Medicine*, vol. 8, pp. 77–85, 2017.
17. M. Penhaker, V. Kasik, and B. Hrvolova, "Advanced Bilirubin Measurement by a Photometric Method," *Electronics and Electrical Engineering*, vol. 19, no. 3, pp. 1–20, 2013.
18. Y. Andreu, "Study of a fluorometric-enzymatic method for bilirubin based on chemically modified bilirubin-oxidase and multivariate calibration," *Talanta*, vol. 57, no. 2, pp. 343–353, 2002.
19. M. Santhosh, S. R. Chinnadayala, A. Kakoti, and P. Goswami, "Selective and sensitive detection of free bilirubin in blood serum using human serum albumin stabilized gold nanoclusters as fluorometric and colorimetric probe," *Biosensors and Bioelectronics*, vol. 59, pp. 370–376, 2014.
20. W. Bian, N. Zhang, and C. Jiang, "Spectrofluorimetric determination of bilirubin in serum samples," *Luminescence*, vol. 26, no. 1, pp. 54–58, 2011.
21. K. Abha et al., "Photoluminescence sensing of bilirubin in human serum using l-cysteine tailored manganese doped zinc sulphide quantum dots," *Sensors and Actuators B Chemical*, vol. 282, pp. 300–308, 2019.
22. L. P. Palilis, A. C. Calokerinos, and N. Grekas, "Chemiluminescence arising from the oxidation of bilirubin in aqueous media," *Analytical Chimica Acta*, vol. 333, no. 3, pp. 267–275, 2016.
23. X. Li and Z. Rosenzweig, "A fiber optic sensor for rapid analysis of bilirubin in serum," *Analytical Chimica Acta*, vol. 353, no. 2–3, pp. 263–273, 2017.
24. J. P. Ndabakuranye et al., "70 years of bilirubin sensing: towards the point-of-care bilirubin monitoring in cirrhosis and hyperbilirubinemia," *Sensors & Diagnostics*, vol. 1, no. 5, pp. 932–954, 2022.
25. M. Martelanc, L. Žiberna, S. Passamonti, and M. Franko, "Application of highperformance liquid chromatography combined with ultra-sensitive thermal lens spectrometric detection for simultaneous biliverdin and bilirubin assessment at trace levels in human serum," *Talanta*, vol. 154, pp. 92–98, 2016.
26. W. Spivak and W. Yuey, "Application of a rapid and efficient h.p.l.c. method to measure bilirubin and its conjugates from native bile and in model bile systems. Potential use as a tool for kinetic reactions and as an aid in diagnosis of hepatobiliary disease," *Biochemical Journal*, vol. 234, no. 1, pp. 101–109, 2016.
27. C. Y. Yeung, Y. S. Fung, and D. X. Sun, "Capillary electrophoresis for the determination of albumin binding capacity and free bilirubin in jaundiced neonates," *Seminars. Perinatology*, vol. 25, no. 2, pp. 50–54, 2001.
28. Z. Nie and Y. S. Fung, "Microchip capillary electrophoresis for frontal analysis of free bilirubin and study of its interaction with human serum albumin," *Electrophoresis*, vol. 29, no. 9, pp. 1924–1931, 2008.
29. H. Sun, Z. Nie, and Y. S. Fung, "Determination of free bilirubin and its binding capacity by HSA using a microfluidic chip-capillary electrophoresis device with a multi-segment circular-ferrofluid-driven micromixing injection," *Electrophoresis*, vol. 31, no. 18, pp. 3061–3069, 2010.
30. U. Chadha et al., "Recent progress and growth in biosensors technology: A critical review," *Journal of Industrial and Engineering Chemistry*, vol. 109, pp. 21–51, 2022.